Fracture mechanics analysis of transverse cracks in thin coatings under spherical Indentation

Herzl Chai
Faculty of Engineering, Tel Aviv University, Israel

ABSTRACT

The competition between transverse cracks originating from the surface and sub-surface of a thin, hard coating bonded by a delamination resistant adhesive to a polycarbonate substrate due to spherical indentation is investigated in real-time as a function of coating thickness and indenter radius. Fine (Y-TZP) and intermediate (alumina) size grain polycrystalline ceramics as well as pre-abraded amorphous glass are used for the coating. As the coating thickness is reduced, the familiar star-shape sub-surface damage is completely suppressed, leaving the surface ring crack to dominate the fracture. In the transition range, the sub-surface damage occurs as a set of *off-axis* circumferential cracks. This observation provides the basis for our simplified treatment of the sub-surface damage as a cylindrical crack.

A linear fracture mechanics approach is used to predict the *onset* of transverse fracture in the coating. In consistency with the tests, the damage on the surface as well as the sub-surface of the coating is assumed as a cylindrical crack. The interactive effect of the coating thickness, indenter radius, crack length and contact radius is explored using a large-strain FEM contact code. In consistency with its polycrystalline nature, the coating is assumed to contain a distribution of cracks. The least fracture load among all permissible crack lengths that is obtained from the analysis is taken as the critical load. The numerical predictions from this analysis compare well with the tests results. The analysis also helps identify the applicability range of a relatively simple critical stress criterion in terms of the system parameters.

INTRODUCTION

The resistance of bi-layer structures to contact damage is of interest in a variety of industrial and technological applications, including tribology (e.g., wear resistance, thermal barrier coatings), bioengineering (e.g., dental crowns, hip prosthesis) and electronic packaging devices. While the fracture behavior depends on a wealth of geometric and material parameters, we focus on *transverse* fracture in a thin, hard coating bonded to a compliant substrate due to spherical indentation. It is generally recognized that the damage in this class of problems is associated with surface ring cracks originating just outside the edge of the contact circle [1-8]. However, because bi-layer structures are generally opaque, the role of the sub-surface damage (i.e., the damage at the lower coating surface) is not readily apparent. To overcome this, a transparent substrate is employed so that the fracture process could be observed in real time from below the sample [5]. The results show that sub-surface damage may occur prior to the surface ring crack even in micron thin coatings. The particular failure mode depends on the geometric and material parameters of the problem, including contact radius, indenter bluntness, coating thickness and likely the size of the grain/flaw in relation to the coating thickness.

There are pressing issues that need to be addressed for a more complete understanding of the damage tolerance of coated structures under spherical indentation. The first is a sound treatment for the sub-surface crack, which is

associated with a three-dimensional fracture pattern. Another challenge is the formulation of a fracture mechanics methodology for nominally uncracked coatings. The problem is particularly acute in polycrystalline ceramics containing a range of grain size that may serve as a crack initiator. Because in indentation problems the largest crack may not necessarily be the detrimental one, the entire range of permissible flaws needs to be considered [9].

Fig. 1 illustrates the specimen configuration used. Three different coating materials are employed, namely soda-lime glass, alumina and Y-TZP. The coating is bonded to a thick polycarbonate substrate via a delamination resistance adhesive. Critical loads to initiate cracks at the surface and the sub-surface of the coating are established from in-situ tests as a function of coating thickness and indenter radius. Based on the test results, a cylindrical crack originating at the sub-surface or surface of the coating is considered. Corresponding fracture initiation loads are established from a FEA that is based on the assumption that cracks of various sizes pre-exist on the coating surfaces.

EXPERIMENTAL

Standard microscopic slides of various thicknesses are used for the glass. The surfaces of the glass are abraded with slurry of 600 SiC particles in order to introduce flaws from which cracks may initiate in a controlled manner [5]. The thickness of the as-received ceramic plates is reduced by means of grinding and polishing down to a sub-micron finish. The coatings are bonded to a clear polycarbonate block by means of a thin (< 10μm), delamination-resistant epoxy adhesive. Hardened steel spheres of various radii (i.e., 0.86mm to 200 mm) are used. Indentations are made at a slow crosshead speed such that fracture occurs within 10 - 30 seconds. The evolution of damage in the coating is observed in-situ from below, i.e., through the substrate, using a video camera that is connected to a zoom telescope (Questar, Inc.). To enhance reflectivity, a thin, semi-transparent film of gold is evaporated on both surfaces of the coating.

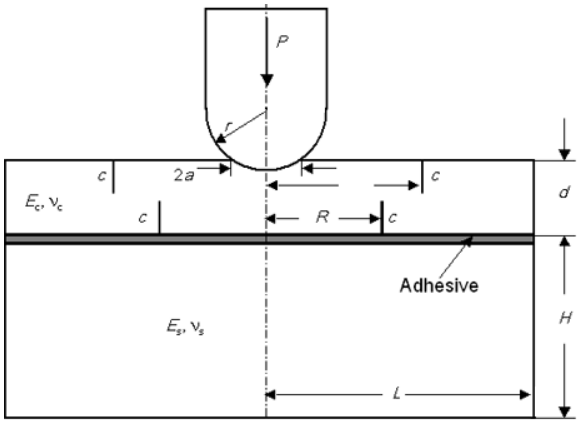

Fig. 1. Schematic of a bi-layer under spherical indentation, including cylindrical cracks emanating from the surface and sub-surface of the coating.

Fig. 2 (symbols) shows critical loads for the alumina/polycarbonate bi-layer, where it is apparent that the sub-surface damage is more detrimental than the surface damage. (It should be noted that the surface damage in these tests occurred *after* the onset of the sub-surface damage). It has been shown that the load needed to initiate a sub-surface crack, in case of very thick coatings, is proportional to square of the coating thickness and inversely proportional to the logarithm of the modulus mismatch ratio, E_c/E_s [5, 10, 11]. The specific relationships among the problem parameters for the two crack systems can be reasonably well approximated as [9]

$$P = A\sigma d^2/\log(BE_c/E_s) \qquad (1)$$

where d is the coating thickness, P is the load, E and σ are Young's modulus and the radial stress at the interface, right on the contact axis, respectively, and the constants (A, B) equal (1.43, 1.2) and (45.5, 62) for the sub-surface and the surface cracks, respectively. The critical load is obtained from Eq. (1) by assigning a critical value σ_F for the peak radial stress.

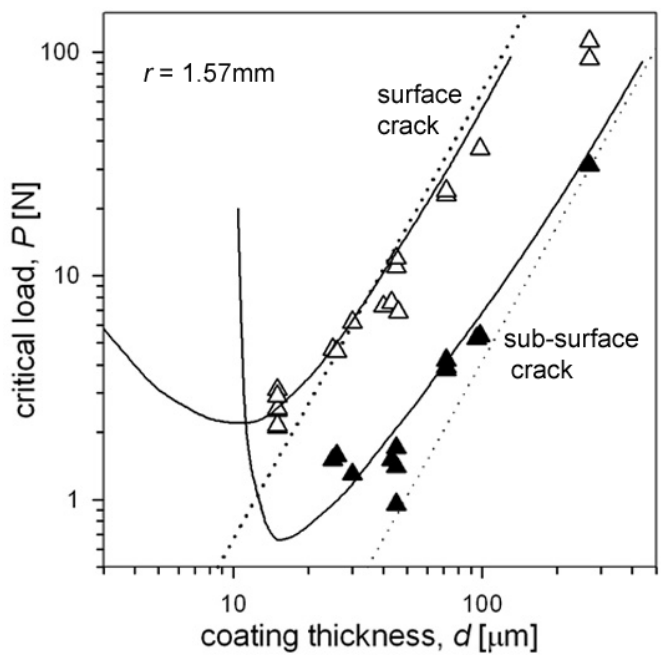

Fig. 2 Critical loads vs. coating thickness for the surface and sub-surface crack systems for alumina/polycarbonate; dotted and solid-line curves are predictions from the linear critical stress criterion and the crack analysis, respectively, while symbols denote test results.

The predictions from Eq. (1) are plotted as dotted lines Fig. 1, where we have assumed σ_F values of 680 MPa and 530 MPa for the sub-surface and the surface crack systems, respectively. As shown, these selections insure a good correlation between the tests and the analytic predictions at relatively large values of *d*, where they apply. (Note that the departure between analysis and tests at large values of *d* in the case of the surface crack is due to the fact that the damage in this case occurred as a second event fracture). Using the common fracture mechanics relations $K_c = \alpha_1 \sigma_F [\pi c_F]^{0.5}$, where c_F denotes the critical crack length, and taking α_1 as 1.1 for the case of the surface crack [12], one gets $c_F = 22$ μm. As shown in Fig. 2, the predictive capability of the simple critical stress criterion is limited to large coating thicknesses. For small values of *d*, a full-fledged fracture analysis seems necessary.

FRACTURE MECHANICS ANALYSIS

The analysis is limited o the *onset* of crack propagation. In the spirit of the thin-film test results [13], a cylindrical crack is assumed for the two coating surfaces, see Fig. 1. Because the coating is brittle, a linearly elastic fracture mechanics approach is considered. In view of the polycrystalline nature of the ceramic coatings, we assume that the coating surface contains a distribution of cracks in the range $0 < c < c_F$, where c_F is the largest flaw in the population, as obtained earlier from the thick coating analysis.

Let K_1 and K_2 be the mode I and the mode II stress intensity factors at the tip of a crack of length *c*. These quantities are evaluated from the FEM nodal displacements according to the following LEFM relation [12]

$$K_i = \frac{E_c u_i}{4(1-\nu_c^{\,2})\sqrt{\Delta / 2\pi}} \ , \ i = 1,2 \qquad (2)$$

where u_1 and u_2 denote the opening and shearing displacements, respectively, on the crack flank, a distance Δ from the crack tip. The load needed to cause crack propagation, P_{cr}, is obtained when the energy release rate, *G*, given as

$$G = (K_1^2 + K_2^2)\,(1-\nu_c^2)/E_c \qquad (3)$$

reach a critical value, G_c. For simplicity, the latter is assumed independent of the mode mix, being equal to the mode I fracture energy, G_{ic}. Using Eqs. (2) and (3), *G* could be determined for a given set of system parameters (i.e., *d*, *c*, *r*, E_c, etc.) as a function of the applied load, *P*. The critical load is obtained when the right hand side of Eq. (3) becomes equal to G_c. To implement this procedure, the crack distance *R* should be specified. Because this quantity is not known in advance, a trial and error scheme is employed; for a given system parameters, results are generated for various values of *R*, with the final choice made on the bases of maximum energy release rate. Figs. 3 show the variation of the critical loads with coating thickness for the alumina/polycarbonate bi-layer, where filled and open symbols correspond to the sub-surface and surface crack, respectively. In all cases, $r = 1.57$ mm. For each crack system, a number of crack lengths are

considered, the largest of which equals c_F. It is apparent that smaller cracks become more detrimental than large ones as d is decreased, but, in the case of the sub-surface crack, this holds true up to $d \approx 3$ μm. The least fracture loads among all possible choices $c < c_F$ ("fracture envelopes") are depicted in Fig. 3 as solid-line curves. The most striking result is perhaps that the sub-surface crack is abruptly suppressed when d becomes sufficiently small (i.e., ~ 15 μm), leaving the surface crack to dominate the strength thereafter. The crack envelopes in Fig. 3 are depicted as solid-line curves in Fig. 2. As shown, the analysis fits reasonably well the tests results.

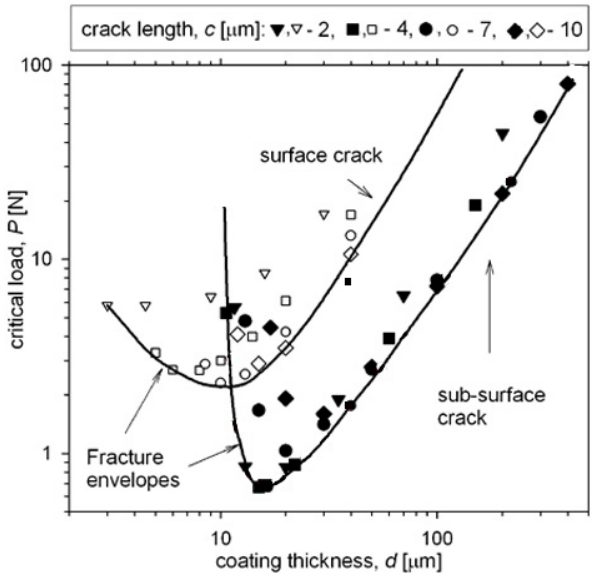

Fig. 3. The variation with coating thickness of the FEM predicted critical loads for an alumina/polycarbonate bi-layer indented by a 1.57mm radius sphere; filled and open symbols correspond to the sub-surface and the surface crack, respectively; solid-line curves are the fracture envelopes.

REFERENCES

1. Diao DF, Kato K, Hokkirigawa K. Journal of Tribology 1994; 116: 860.
2. Anderson R, Toth G, Gan L, Swain MV. Engineering Fracture Mechanics 1998; 61: 93.
3. Hainsworth SV, McGurk MR, Page TF. Surface and Science technology 1998; 102:97.
4. Wang JS, Sugimura Y, Evans AG, Tredaway WK. Thin Solid Films 1998; 325: 163.
5. Chai H, Lawn BR, Wuttiphan S. Journal of Material Research 1999; 14:3805.
6. Michler J, Tobler M, Blank E. Diamond and Related Materials 1999; 8:510.
7. Begley MR, Evans AG, Hutchinson JW. International Journal of Solids and Structures 1999; 36: 2773.

8. Souza RM, Sinatora A, Mustoe GGW, Moore J. Wear 2001; 251: 1337.
9. Chai H. International Journal of Fracture 2003; 119: 263.
10. Rhee YW, Kim HW, Deng Y, Lawn BR. Journal of the American Ceramic Society 2001; 84: 1066.
11. Miranda P, Pajares A, Guiberteau F, Cumbrera FL, Lawn BR. Journal of Materials research 2001; 16:115.
12. Lawn BR. Fracture of Brittle Solids, Second Edition, Cambridge University Press, 1995.
13. Chai, H, Lawn, BR. Journal of Material Research 2004, in press.